Nitrite Reduction by Myoglobin in Surfactant Films

Rong Lin, Mekki Bayachou, John Greaves, and Patrick J. Farmer*

Department of Chemistry, University of California, Irvine Irvine, California 92697-2025

Received July 28, 1997
Revised Manuscript Received October 23, 1997

Nitrite reductases (NiR) are a widespread class of enzymes which perform integral steps in the biochemical cycling of nitrogen.[1−3] Three different porphyrinoid active sites have been characterized in NiR: isobacteriochlorin in siroheme NiR,[1] dioxoisobacteriochlorin in the heme cd_1 NiR,[2] and porphyrin in hexaheme NiR.[3] Both the siroheme and hexaheme enzymes catalyze the multi-electron, proton coupled reduction of NO_2^- to NH_4^+, eq 1. The heme cd_1 NiR participate in multienzyme denitrification processes which result in products including the N−N coupled gases N_2O and N_2, eq 2.[4] All known NiR have associated redox factors, (e.g., the Fe_4S_4 cluster bound to the siroheme in the assimilatory NiR) which serve to funnel electrons into the active site.

$$NO_2^- + 6e^- + 8H^+ \rightarrow NH_4^+ + 2H_2O \quad (1)$$

$$NO_2^- \xrightarrow{[e^-]} NO + N_2O + N_2 + ... \quad (2)$$

Electrochemical nitrite reduction has been demonstrated for water-soluble Fe-porphyrin[5] and other transition metal complexes.[6] Similar unmediated electrocatalysis by proteins is difficult to characterize because of their generally poor voltammetric response.[7,8] Nassar and Rusling have shown the electrochemical response of the single-heme protein myoglobin (Mb) is greatly enhanced in surfactant films.[9,10] Layered films of surfactants such as dimethyldidodecylammonium bromide (ddab) on pyrolytic graphite (PG) adsorb Mb from solution, and spectroscopic analysis of Mb/ddab films on transparent supports confirms the native protein structure is maintained in this unique environment.[11] Such Mb/ddab films formed on PG electrodes yield electrochemistry assignable to Mb *(vide infra)* when immersed in aqueous solution.[9−11] We herein report that these electroactive Mb/ddab films act as efficient catalysts for the biomimetic reduction of nitrite, yielding products characteristic of both enzymatic reactivities.

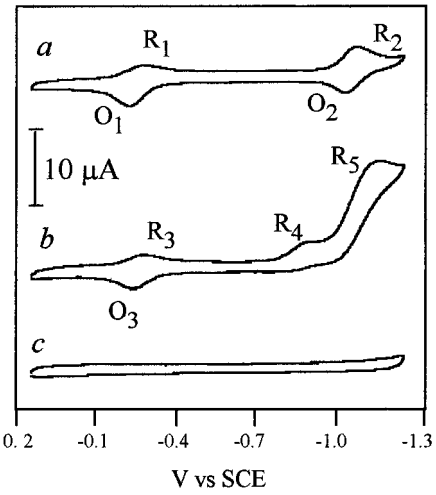

Figure 1. Cyclic voltammograms in deareated pH 7.4 buffer (50 mM NaBr, 500 mV/s) of (a) the Mb/ddab film electrode, (b) the Mb/ddab film with 3 mM $NaNO_2$, (c) and the ddab film electrode with 3 mM $NaNO_2$.

Typical cyclic voltammograms of Mb/ddab cast on PG display two reduction couples in pH 7 buffered solutions, Figure 1a.[12,13] The first, R_1/O_1, $E^{\circ\prime}$ at −221 mV vs SCE, is assigned to the $Fe^{III/II}$ couple of Mb;[9] the second couple, R_2/O_2 at −1093 mV, is tentatively assigned to $Fe^{II/I}$.[10a] The presence of nitrite in the bulk solution (Figure 1b) dramatically changes the current response of the electrode; the $Fe^{III/II}$ couple (R_3/O_3 at −235 mV) shifts to lower potentials indicative of nitrite binding at the redox-active Fe site. In addition, two new catalytic waves are present, labeled R_4 (−895 mV) and R_5 (−1205 mV), which are not seen in the absence of Mb in the ddab films (Figure 1c). The increased current flow indicates multiple electrons passed per Mb, i.e., catalytic turnover. Increasing the nitrite concentration results in a rise in the catalytic current up to a limiting value; such saturation behavior is characteristic of enzyme catalysis.[14] Analysis of current at R_5 vs substrate concentration yields a Michaelis constant, K_m, of 2.3 mM, close to the K_d of 3.3 mM found for nitrite binding to ferric Mb in solution.[15]

The pH dependence of the catalysis is shown in Figure 2a. At pH 5.1, under quasi-steady-state conditions (20 mV/s), the peak current ratios are ca. 20 for R_4 and ca. 220 for R_5 vs the noncatalytic $Fe^{III/II}$ reduction peak, R_3. As the pH is raised to 9, the catalytic peaks (R_4 and R_5) shift to more negative potentials and the currents decrease as expected for proton-

(1) Guerrero, M. G.; Vega, J. M.; Losada, M. *Annu. Rev. Plant Physiol.* **1981**, *32*, 169.
(2) Hochstein, L. I.; Tomlinson, G. A. *Annu. Rev. Microbiol.* **1988**, *42*, 231.
(3) Brittain, T.; Blackmore, R.; Greenwood, C.; Thomson, A. J. *Euro. J. Biochem.* **1992**, *209*, 793.
(4) (a) Averill, B. A. *Chem. Rev. (Washington, D.C.)* **1996**, *96*, 2951. (b) Ye, R. W.; Averill, B. A.; Tiedje, J. M. *Appl. Environ. Microbiol.* **1994**, *60*, 1053.
(5) (a) Murphy, W. R., Jr.; Takeuchi, K.; Barley, M. H.; Meyer, T. J. *J. Am. Chem. Soc.* **1982**, *104*, 5817. (b) Barley, M. H.; Takeuchi, K.; Meyer, T. J. *J. Am. Chem. Soc.* **1986**, *108*, 5876. (c) Barley, M. H.; Rhodes, M. R.; Meyer, T. J. *Inorg. Chem.* **1987**, *26*, 1746. (d) Younathan, J. N.; Wood, K. S.; Meyer, T. J. *Inorg. Chem.* **1992**, *31*, 3280.
(6) (a) Toth, J. E.; Anson, F. C. *J. Am. Chem. Soc.* **1989**, *111*, 2444. (b) Rhodes, M. R.; Barley, M. H.; Meyer, T. J. *Inorg. Chem.* **1991**, *30*, 629. (c) Sunohara, S.; Nishimura, K.; Yahikozawa, K.; Ueno, M.; Eny, M.; Takasu, Y. *J. Electroanal. Chem.* **1993**, *354*, 161. (d) Keita, B.; Belhouari, A.; Nadjo, L.; Constant, R. *J. Electroanal. Chem.* **1995**, *381*, 243.
(7) (a) Guo, L.-H.; Hill, H. A. O. *Adv. Inorg. Chem.* **1991**, *36*, 341. (b) Hawkridge, F. M.; Taniguchi, I. *Comments Inorg. Chem.* **1995**, *17*, 163. (c) Hill, H. A. O. *Coord. Chem. Rev.* **1996**, *151*, 115.
(8) (a) Armstrong, F. A.; Butt, J. N.; Sucheta, A. *Meth. Enzymol.* **1993**, *227*, 479. (b) Hirst, J.; Sucheta, A.; Ackrell, B. A. C.; Armstrong, F. A. *J. Am. Chem. Soc.* **1996**, *118*, 5031. (c) Crumbliss, A. L.; Stonehuerner, J.; Henkens, R. W.; O'Daly, J. P.; Zhao, J. *New J. Chem.* **1994**, *18*, 327.
(9) (a) Rusling, J. F.; Nassar, A. E. F. *J. Am. Chem. Soc.* **1993**, *115*, 11891. (b) Nassar, A. E. F.; Willis, W. S.; Rusling, J. F. *Anal. Chem.* **1995**, *67*, 2386.
(10) (a) Nassar, A. E. F.; Bobbitt, J. M.; Stuart, J. D.; Rusling, J. F. *J. Am. Chem. Soc.* **1995**, *117*, 10986. (b) Nassar, A.-E.; Zhang, Z.; Hu, N.; Rusling, J. F.; Kumosinski, T. F. *J. Phys. Chem.* **1997**, *101*, 2224.
(11) (a) Rusling, J. F.; Nassar, A. E. F.; Kumosinski, T. F. *ACS Symp. Ser.* **1994**, *576*, 250. (b) Nassar, A. E. F.; Zhang, Z.; Chynwat, V.; Frank, H. A.; Rusling, J. F.; Suga, K. *J. Phys. Chem.* **1995**, *99*, 11013. (c) Nassar, A. E. F.; Narikiyo, Y.; Sagara, T.; Nakashima, N.; Rusling, J. F. *J. Chem. Soc., Faraday Trans.* **1995**, *91*, 1775.
(12) Horse skeletal myoglobin (Sigma) and ddab (Aldrich) films were cast as in ref 9a onto homemade electrodes made of basal-plane, pyrolytic graphite discs (Union Carbide) sealed with epoxy into glass tubes. For typical preparations the surface coverage of electroactive Mb was 1.5×10^{-9} mol/cm^2 as measured by steady-state coulometry (5 mV/s scan rates). All potentials are referenced vs SCE.
(13) The irreversibility of R_1/O_1 at scan rates above 20 mV/s is due, we believe, to slow dissociation of Fe-bound water upon reduction: (a) Farmer, P. J.; Lin, R.; Bayachou, M. *Comments Inorg. Chem.* In press. (b) Van Dyke, B. P.; Saltman, P.; Armstrong, F. A. *J. Am. Chem. Soc.* **1996**, *118*, 3490.
(14) Lineweaver−Burke plot given in the Supporting Information.
(15) Sono, M.; Dawson, J. H. *J. Biol. Chem.* **1982**, *257*, 5496.
(16) The R_1/O_1 couple is itself pH dependent, ref 10b. Further studies are in progress to delineate the complex pH dependences. Bard, A. J.; Faulkner, L. R. *Electrochemical Methods-Fundamentals and Applications*; Wiley: New York, 1980; pp 455−461.

S0002-7863(97)02529-8 CCC: $14.00

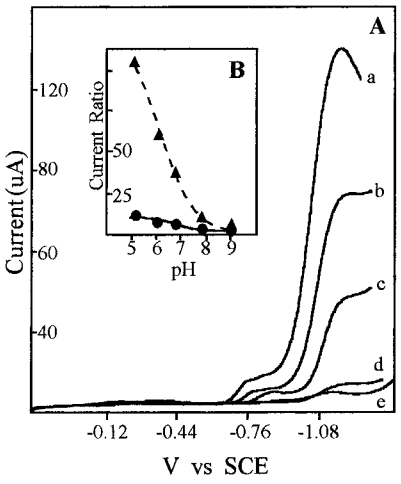

Figure 2. pH dependence of catalytic waves R_4 and R_5. (A) Linear sweep voltamograms (100 mV/s) of Mb/ddab/PG electrodes in 10 mM $NaNO_2$ at varying pH solutions: (a) 5.1, (b) 6.0, (c) 6.8, (d) 7.8, and (e) 9.0. (B) Peak current ratio dependence on pH: ● = $i_p(R_4)/i_p(R_1)$; ▲ = $i_p(R_5)/i_p(R_1)$.

coupled processes. At pH >9 there is no current above that expected for Mb reduction, R_2. The effect of pH on the two catalytic waves is distinct. The potential of R_5 has a smaller pH dependence than that of R_4 (−20 mV vs −45 mV per pH unit) and its current a larger pH dependence, shown in Figure 2 inset, indicating the second catalytic wave encompasses a multielectron, multiproton process.[16]

To identify the products of the catalysis, bulk electrolysis of nitrite solutions at pH 5.5 was performed at the R_5 potential.[17] Analysis of the electrolysis solution after 2 h showed 25% NH_4^+ and 17% NH_3OH^+ are produced from the nitrite consumed.[18] The total of the aqueous products identified never accounts for more than 60% of the nitrite consumed during electrolysis. To test for gaseous products, the headgas over bulk electrolysis experiments using ^{15}N-labeled nitrite was continuously monitored by mass spectrometry, Figure 3.[19] A strong signal of $[^{15}N_2O]^+$ (*m*/*z* 46) ions was seen after 5 min and abundances for $[^{15}N_2]^+$ (*m*/*z* 30) and $[^{15}NO]^+$ (*m*/*z* 31) in excess of that expected from $[^{15}N_2O]^+$ fragmentation were seen.[20] While the normalized time trace for $[^{15}NO]^+$ follows that of $[^{15}N_2O]^+$, the envelope for $[^{15}N_2]^+$ suggests its formation at an independent rate. Previous reports of the formation of N_2O and N_2 in model systems invoked a bimolecular coupling of Fe nitrosyl or nitrido complexes;[5b,d] such coupling is unlikely to occur at isolated Mb active sites. Gas analysis at varied electrolysis potentials shows that $^{15}N_2O$ production commences at the R_4 catalytic wave; thus the characteristic denitrification reaction occurs upon reduction of the ferrous-Mb nitrite complex in this system.[21]

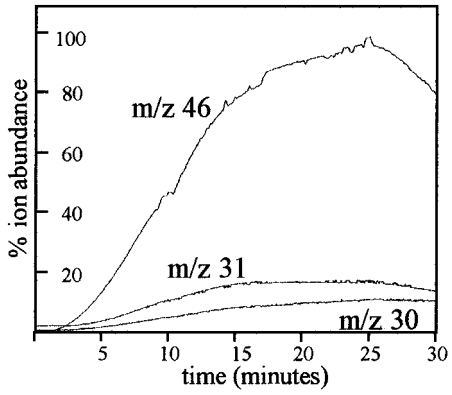

Figure 3. Mass chromatograms of *m*/*z* 46 = $[^{15}N_2O]^+$, *m*/*z* 31 = $[^{15}NO]^+$, and *m*/*z* 30 = $[^{15}N_2]^+$ from continuously sampled headgas over bulk electrolysis of a 14 mM $Na^{15}NO_2$ solution, pH 5.5, using the Mb/ddab/PG electrode at −1.2 V SCE.

Several sequential reduction pathways have been proposed for nitrite reduction to ammonia by the assimilatory NiR enzymes.[5b,22,23] Likewise, the mechanism and nature of the precursor to N−N coupled products in the dissimilatory enzymes have been much debated.[3,24] We are now pursuing mechanistic studies with the Mb/ddab/PG catalyst, a system in which both enzymatic reactivities are achieved under conditions where potential and current flow data can be matched to product formation within an isolated protein site.

Acknowledgment. This research was supported by the National Science Foundation (CHE-9629938) and startup funds from the University of California, Irvine.

Supporting Information Available: Plots of current vs scan rate for the R_1/O_1 couple, a determination of the heterogeneous rate constant, a Lineweaver−Burke plot of catalytic current vs nitrite concentration, and a time trace of the potential dependence of $^{15}N_2O$ production during electrolysis (3 pages). See any current masthead page for ordering and Internet access instructions.

JA972529A

(17) Bulk electrolysis experiments utilized pyrolytic graphite plates (1.0 × 1.0 × 0.2 cm) coated on one side with Mb/ddab. The other side was connected to a wire with Ag paste and sealed with epoxy. Solutions of degassed 0.2 M acetate pH 5.5 buffer with 0.05 M NaBr added as electrolyte were used; $Na^{15}NO_2$ (Isotec) concentrations were typically 10 mM. Controlled potential was applied by using a BAS 100W and a Power Module potentiostat, a SCE reference, and a Pt grid counter electrode separated by a fine frit from the main compartment.

(18) Colorimetric determinations of solution-based products were conducted as in the following references. (a) Nitrite: Jeffery, G. H.; Bassett, J.; Mendham, J.; Denney, R. C. *Vogel's Textbook of Quantitative Chemical Analysis*, 5th ed.; Longman Scientific & Technical, 1989; p 702. (b) Hydroxylamine: Frear, D. S.; Burell, R. C. *Anal. Chem.* **1955**, *27*, 1664. (c) Ammonia: Liu, M.; Costa, C.; Moura, I. *Meth. Enzymol.* **1994**, *243*, 303.

(19) Mass spectroscopy experiments utilized a gastight cell. A continuous He purge transferred the headgas directly into a Micromass Autospec mass spectrometer via a fused silica line. Data were acquired in EI mode at 1000 resolution. Subsequent determinations used a gas trapping loop and a PLOT GC column (fused silica 50 m × 0.32 mm − coating = Al_2O_3, KCl).

(20) Both $[^{15}NO]^+$ and $[^{15}N_2]^+$ are produced by $^{15}N_2O$ ionization in the MS, but varying abundance ratios measured during electrolysis deviated substantially from those obtained by ionization of an authentic $^{15}N_2O$ sample. Separation of sampled headgas aliquots by a GC column prior to ionization confirms independent ^{15}NO and $^{15}N_2$ production during electrolysis. Corrected production ratios from gas chromatograph peak areas give $^{15}N_2$:^{15}NO:$^{15}N_2O$ ca. 1:2:17 after an hour of electrolysis.

(21) A mass chromatogram, as in Figure 3, of bulk electrolysis of $Na^{15}NO_2$ solution, pH 5.5, using the Mb/ddab/PG electrode at varied potentials is provided in the Supporting Information.

(22) (a) Lui, S. M.; Liang, W.; Soriano, A.; Cowan, J. A. *J. Am. Chem. Soc.* **1994**, *116*, 4531. (b) Lui, S. M.; Liang, W.; Soriano, A.; Cowan, J. A. *J. Am. Chem. Soc.* **1993**, *115*, 10483.

(23) Liu, Y.; Ryan, M. D. *J. Electroanal. Chem.* **1994**, *368*, 209.

(24) (a) Ferguson, S. J. *Antonie van. Leeuwenhoek* **1994**, *66*, 89. (b) Henry, Y.; Bessieres, P. *Biochimie* **1984**, 66, 259.